Preprint ANL/MCS-P5199-0914

Nonlinear Compact Finite-Difference Schemes with Semi-Implicit Time Stepping

Debojyoti Ghosh and Emil M. Constantinescu

Abstract Atmospheric flows are characterized by a large range of length scales as well as strong gradients. The accurate simulation of such flows requires numerical algorithms with high spectral resolution, as well as the ability to yield nonoscillatory solutions across regions of high gradients. These flows exhibit a large range of time scales as well—the slowest waves propagate at the flow velocity and the fastest waves propagate at the speed of sound. Time integration with explicit methods are thus inefficient and algorithms with semi-implicit time integration have been successfully used in past studies. We propose a finite-difference method for atmospheric flows that uses a weighted compact scheme for spatial discretization and the implicit-explicit additive Runge-Kutta methods for time integration. We present results for benchmark atmospheric flows and compare our results with existing ones in the literature.

1 Introduction

The simulation of atmospheric flows requires accurate numerical solutions to the compressible Navier-Stokes equations or the inviscid Euler equations if the physical viscosity and heat conduction are neglected. Such flows are characterized by localized flow structures and strong gradients, and numerical algorithms need a high spectral resolution and must be nonoscillatory across regions of strong gradients. Past and present algorithms used for numerical weather prediction include finite-difference methods [13], finite-volume methods [1], as well as discontinuous Galerkin and spectral element methods [10, 9]. Although standard finite-difference methods suffer from poor spectral resolution, compact finite-difference methods

Debojyoti Ghosh
Mathematics & Computer Science Division, Argonne National Laboratory, Argonne, IL, United States e-mail: ghosh@mcs.anl.gov

Emil M. Constantinescu
Mathematics & Computer Science Division, Argonne National Laboratory, Argonne, IL, United States e-mail: emconsta@mcs.anl.gov

[15] have significantly higher spectral resolution and have been applied to applications such as large eddy simulations (LES) and direct numerical simulations (DNS) of turbulent flows [14, 18].

In this study, we propose a high-order finite-difference method for atmospheric flows based on the compact-reconstruction weighted essentially nonoscillatory (CRWENO) schemes [5, 6, 8]. The CRWENO schemes combine the high spectral resolution of linear compact schemes with the solution-dependent stencil adaptation method of the WENO schemes [17, 11] to yield nonoscillatory solutions. They are thus well suited for the simulation of atmospheric flows. We explore implicit-explicit time-integration schemes based on a separation of stiff and non-stiff components of the governing equations [10]. We present results for a benchmark atmospheric flow problem.

2 Governing Equations

We consider the conservative form of the Euler equations based on the mass, momentum and potential temperature for meso-scale flows (neglecting the Coriolis forces) [10]. These are given by,

$$\frac{\partial}{\partial t}\begin{bmatrix}\rho' \\ \rho\mathbf{u} \\ \rho\theta\end{bmatrix} + \nabla\cdot\begin{bmatrix}\rho\mathbf{u} \\ \rho\mathbf{u}\otimes\mathbf{u} + p'\mathscr{I} \\ \rho\theta\mathbf{u}\end{bmatrix} = \begin{bmatrix}0 \\ -\rho' g\hat{\mathbf{k}} \\ 0\end{bmatrix} \tag{1}$$

where ρ is the density, $\mathbf{u}$ is the velocity vector, p is the pressure, $\mathscr{I}$ is the identity matrix, and g is the acceleration due to gravity acting along the z-axis of the coordinate system with unit vector $\hat{\mathbf{k}}$. The potential temperature θ is given by,

$$\theta = \frac{T}{\pi};\ \pi = \left(\frac{p}{p_0}\right)^{\frac{R}{C_P}} \tag{2}$$

where T is the temperature, π is the Exner pressure, p_0 is the pressure at the surface (or reference altitude), R is the universal gas constant, and C_P is the constant pressure specific heat. The system of equations is completed by the equation of state, $p = p_0\left(\frac{\rho R\theta}{p_0}\right)^{\frac{C_P}{C_V}}$, where C_V is the constant volume specific heat. Equation (1) are expressed in terms of the density, pressure, and potential temperature perturbations (ρ', p', θ') that can be expressed as $(\cdot)' = (\cdot)(x,y,z,t) - \bar{(\cdot)}(z)$, where $\bar{(\cdot)}$ is the mean density, pressure or potential temperature in hydrostatic balance $C_P\bar{\theta}\frac{d\bar{\pi}}{dz} = -g$. The governing equations form a system of hyperbolic partial differential equations (PDE) and are solved by a conservative finite-difference algorithm.

3 Numerical Methodolgy

Equation (1) can be expressed as a system of hyperbolic conservation laws with a source term,

$$\frac{\partial \mathbf{U}}{\partial t} + \frac{\partial \mathbf{f}_i(\mathbf{U})}{\partial x_i} = \mathbf{s}(\mathbf{U}),\ i = 1,\cdots,D, \tag{3}$$

where $\mathbf{U}$ is the solution, $\mathbf{f}_i$ is the flux along the i-th dimension, $\mathbf{s}$ is the source term, and D is the number of dimensions. We describe the discretization of (3) in one dimension ($D=1$); it can be trivially extended to multiple dimensions. A conservative, finite-difference spatial discretization of (3) on this grid results in a semi-discrete ordinary differential equation (ODE) in time,

$$\frac{d\mathbf{U}_j}{dt} + \frac{1}{\Delta x}\left[\hat{\mathbf{f}}_{j+1/2} - \hat{\mathbf{f}}_{j-1/2}\right] = \mathbf{s}_j,\ j = 1,\cdots,N, \tag{4}$$

where j denotes the grid index, $\mathbf{U}_j = \mathbf{U}(x_j)$ is the cell-centered solution, $\hat{\mathbf{f}}_{j+1/2}$ is the numerical flux at the cell interface $x_{j+1/2}$, and $\mathbf{s}_j$ is the source term evaluated at the cell center.

3.1 Reconstruction

We use the CRWENO scheme [5, 6, 8] to reconstruct the interface fluxes $\hat{\mathbf{f}}_{j+1/2}$ from the cell-centered flux $\mathbf{f}_j$. We briefly summarize the scheme in this section; a more complete description is available in [5]. The fifth-order CRWENO scheme (CRWENO5) is constructed by considering three third-order accurate compact interpolation schemes for the flux function at the $(j+1/2)$-th interface,

$$\frac{2}{3}\hat{f}_{j-1/2} + \frac{1}{3}\hat{f}_{j+1/2} = \frac{1}{6}\left(f_{j-1} + 5f_j\right);\quad c_1 = \frac{2}{10}, \tag{5}$$

$$\frac{1}{3}\hat{f}_{j-1/2} + \frac{2}{3}\hat{f}_{j+1/2} = \frac{1}{6}\left(5f_j + f_{j+1}\right);\quad c_2 = \frac{5}{10}, \tag{6}$$

$$\frac{2}{3}\hat{f}_{j+1/2} + \frac{1}{3}\hat{f}_{j+3/2} = \frac{1}{6}\left(f_j + 5f_{j+1}\right);\quad c_3 = \frac{3}{10}. \tag{7}$$

Multiplying (5)—(7) with their optimal coefficients ($c_k,\ k = 1,2,3$) and adding, we obtain the fifth-order accurate compact interpolation scheme,

$$\frac{3}{10}\hat{f}_{j-1/2} + \frac{6}{10}\hat{f}_{j+1/2} + \frac{1}{10}\hat{f}_{j+3/2} = \frac{1}{30}f_{j-1} + \frac{19}{30}f_j + \frac{1}{3}f_{j+1}. \tag{8}$$

We now compute weights ω_k based on the local smoothness of the solution [11] such that they converge to the corresponding optimal coefficient c_k when the solution is locally smooth, and approach zero at or near a discontinuity. They can be expressed as:

$$\omega_k = \frac{\alpha_k}{\sum_k \alpha_k}; \; \alpha_k = \frac{c_k}{(\varepsilon + \beta_k)^p}; \; k = 1,2,3, \tag{9}$$

where $\varepsilon = 10^{-6}$ is a small number to prevent division by zero. The smoothness indicators (β_k) measure the local smoothness of the solution and are given by,

$$\beta_1 = \frac{13}{12}(f_{j-2} - 2f_{j-1} + f_j)^2 + \frac{1}{4}(f_{j-2} - 4f_{j-1} + 3f_j)^2, \tag{10}$$

$$\beta_2 = \frac{13}{12}(f_{j-1} - 2f_j + f_{j+1})^2 + \frac{1}{4}(f_{j-1} - f_{j+1})^2, \tag{11}$$

$$\text{and } \beta_3 = \frac{13}{12}(f_j - 2f_{j+1} + f_{j+2})^2 + \frac{1}{4}(3f_j - 4f_{j+1} + f_{j+2})^2. \tag{12}$$

Multiplying (5)—(7) with ω_k instead of c_k and adding, we obtain the CRWENO5 scheme,

$$\left(\frac{2}{3}\omega_1 + \frac{1}{3}\omega_2\right)\hat{f}_{j-1/2} + \left[\frac{1}{3}\omega_1 + \frac{2}{3}(\omega_2 + \omega_3)\right]\hat{f}_{j+1/2} + \frac{1}{3}\omega_3\hat{f}_{j+3/2} = \frac{\omega_1}{6}f_{j-1} + \frac{5(\omega_1 + \omega_2) + \omega_3}{6}f_j + \frac{\omega_2 + 5\omega_3}{6}f_{j+1}. \tag{13}$$

The resulting scheme is fifth-order accurate when the solution ($\omega_k \to c_k$) is smooth, and yields nonoscillatory solution across discontinuities by biasing the interpolation stencil away from it. Equation (13) requires the solution to a tridiagonal system of equations at each time-integration step or stage; however past studies [5] demonstrated the higher computational efficiency of the CRWENO scheme compared with a standard finite-difference scheme. A scalable and efficient parallel implementation of the CRWENO5 scheme is discussed in [7]. The above discussion describes the left-biased computation of the interface flux; the corresponding expressions for the right-biased interface flux can be similarly obtained. The final flux at a given interface is computed from the left- and right-biased approximations using the Rusanov upwinding scheme [16].

3.2 Time Integration

Equation (4) is integrated in time using explicit Runge-Kutta (ERK) and implicit-explicit additive Runge-Kutta (ARKIMEX) methods. Efficient implementations of these methods are available in the `TS` (time stepping) module of `PETSc` [3, 4]. ERK methods are often inefficient because the time step size is restricted by the acoustic (fastest) wave. Implicit-explicit time-integration methods have been previously applied to atmospheric flows [10, 9]. We briefly summarize the separation of stiff and non-stiff components of the governing equations and its implicit-explicit discretization in time.

Equation (1) can be rearranged such that the right-hand side comprises a non-stiff term and a linear stiff term [10],

$$\frac{\partial \mathbf{U}}{\partial t} = \mathbf{S}(\mathbf{U}) + \mathbf{L}(\mathbf{U}), \tag{14}$$

$$\mathbf{U} = \begin{bmatrix} \rho' \\ \rho\mathbf{u} \\ \rho\theta' \end{bmatrix}, \ \mathbf{S}(\mathbf{u}) = -\nabla\cdot \begin{bmatrix} 0 \\ \rho\mathbf{u}\otimes\mathbf{u} \\ \rho\theta\mathbf{u} - \rho\bar{\theta}\mathbf{u} \end{bmatrix}, \ \mathbf{L}(\mathbf{u}) = -\begin{bmatrix} \nabla\cdot\rho\mathbf{u} \\ \nabla p' + g\rho'\hat{\mathbf{k}} \\ \nabla\cdot\rho\bar{\theta}\mathbf{u} \end{bmatrix},$$

where the pressure perturbation is linearized as $p' = \frac{\gamma\bar{p}}{\bar{\rho}\bar{\theta}}\left(\rho\theta - \bar{\rho}\bar{\theta}\right)$, with $\gamma = C_P/C_V$ as the specific heat ratio. The non-stiff component, $\mathbf{S}(\mathbf{U})$, of the right-hand side of (14) consists of the entropy waves while the linear stiff component, $\mathbf{L}(\mathbf{U})$, consists of the acoustic and gravity waves. Equation (14) is spatially discretized and integrated in time using the ARKIMEX methods [2, 12, 19] where an ERK method is applied to the non-stiff term, while an ARK method is applied to the stiff term. This multistage procedure can be expressed as follows,

$$\mathbf{U}^{(k)} = \mathbf{U}_n + \Delta t \sum_{i=1}^{k-1} a_{ki}\hat{\mathbf{S}}\left(\mathbf{U}^{(i)}\right) + \Delta t \sum_{i=1}^{k} \tilde{a}_{ki}\hat{\mathbf{L}}\left(\mathbf{U}^{(i)}\right), \ k = 1,\cdots,s, \tag{15}$$

$$\mathbf{U}_{n+1} = \mathbf{U}_n + \Delta t \sum_{i=1}^{s} b_i\hat{\mathbf{S}}\left(\mathbf{U}^{(i)}\right) + \Delta t \sum_{i=1}^{s} \tilde{b}_i\hat{\mathbf{L}}\left(\mathbf{U}^{(i)}\right), \tag{16}$$

where s is the number of stages, the superscripts of $\mathbf{U}$ indicate the stage index, and the subscripts of $\mathbf{U}$ indicate the time step. The coefficients a_{ki}, and b_i specify the ERK method, and the coefficients $\tilde{a}_{ki}$ and $\tilde{b}_i$ specify the ARK method. $\hat{\mathbf{S}}$ and $\hat{\mathbf{L}}$ are the spatially discretized forms of $\mathbf{S}(\mathbf{U})$ and $\mathbf{L}(\mathbf{U})$ respectively.

Past applications of implicit-explicit time-integration to atmospheric flows [10, 9] used the discontinuous Galerkin or the spectral element methods for the discretization of spatial derivatives; this resulted in (15) being a linear system. We, however, use a nonlinear finite-difference operator to discretize the spatial derivative, as given by (4) and (13). Thus, $\hat{\mathbf{L}}$ is nonlinear even though $\mathbf{L}$ is linear, and (15) is a nonlinear system of equations. We make two comments on our algorithm in this context.

- We ensure that the discretized right-hand side $(\hat{\mathbf{S}} + \hat{\mathbf{L}})$ is consistent with the right-hand side of (14) by using the *same* finite-difference operator to discretize both $\mathbf{S}$ and $\mathbf{L}$. The nonlinear weights in (13) are computed based on the smoothness of $\mathbf{S} + \mathbf{L}$, and the resulting CRWENO5 scheme is applied to both terms.
- We linearize the finite-difference operator at each stage such that (15) is a linear system of equations. We compute the nonlinear weights in (13) at the beginning of stage k based on the smoothness of $(\mathbf{S}+\mathbf{L})\left(\mathbf{U}^{(k-1)}\right)$ (or $(\mathbf{S}+\mathbf{L})(\mathbf{U}_n)$ for $k = 1$) and solve (15) as a linear system (since, once the nonlinear weights are fixed, (13) is a linear operator).

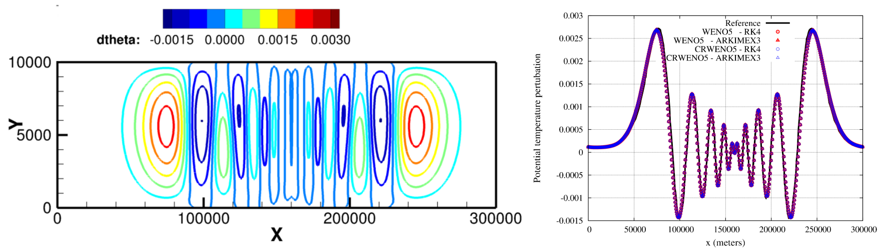

(a) Potential temperature perturbation contours

(b) Cross-sectional variation of potential temperature perturbation

Fig. 1 Solutions of the inertia-gravity wave problem obtained on a grid with 1200×50 points.

4 Results

We verify our algorithm by solving the two-dimensional inertia-gravity wave problem, a benchmark problem in atmospheric flows [13]. The domain is a periodic channel with dimensions $300,000 \times 10,000$ meters. Zero-flux boundary conditions are specified at the top and bottom boundaries. The initial atmosphere has a mean flow of 20 meters/second and is uniformly stratified with a Brunt-Vaisala frequency of $\mathscr{N} = 0.01$/second [10, 13]. A perturbation in the potential temperature is introduced as,

$$\theta' = \theta_c \frac{\sin\left(\frac{\pi_c z}{h_c}\right)}{1 + \left(\frac{x - x_c}{a_c}\right)^2}, \tag{17}$$

where $\theta_c = 0.01$ Kelvin, $h_c = 10,000$ meters, $a_c = 5000$ meters, $x_c = 100,000$ meters, and π_c is the trigonometric constant. Solutions are obtained at a final time of 3000 seconds.

Figure 1(a) shows the potential temperature perturbation (θ') contours for a solution obtained with the CRWENO5 scheme on a grid with 1200×50 points. The solution is integrated in time with the second-order accurate, two-stage ARKIMEX 2C method at a CFL of 8. We observe a good agreement with results in the literature [1, 10, 13]. The cross-sectional variation of the potential temperature perturbation through $z = 5000$ meters is shown in figure 1(b) for the solutions obtained with the CRWENO5 as well as the fifth-order WENO (WENO5) [11] schemes. The explicit four-stage, fourth-order Runge-Kutta (RK4) and the three-stage, third-order ARKIMEX (ARKIMEX3) methds are used to integrate the solution in time. An excellent agreement is observed for all the methods with the reference solution, obtained using the spectral element method with 10^{th} order polynomials and 250 meters grid resolution [10].

The convergence and conservation properties of our algorithm are evaluated by obtaining solutions on a fine grid with 8192×256 points. Figure 2(a) shows the L_2 norm of the error as a function of the time step sizes. The reference solution

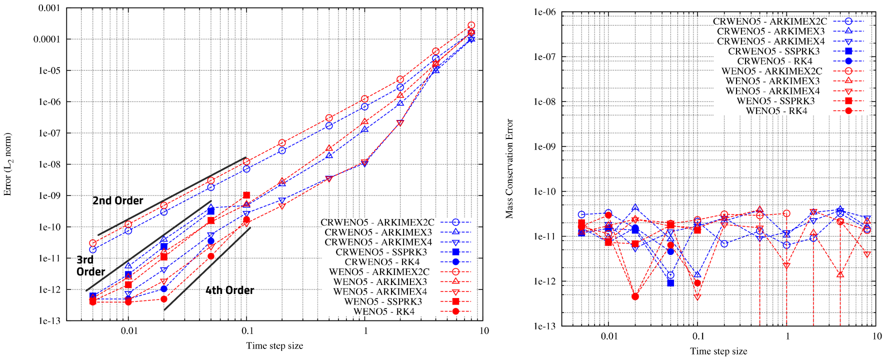

(a) L_2 norm of the error as a function of time step size (b) Mass conservation error as a function of time step size

Fig. 2 Error analysis on a grid with 8192×256 points.

is computed with the strong-stability-preserving three-stage, third-order Runge-Kutta (SSPRK3) scheme and a small time step size of 0.0005. We consider two ERK schemes, SSPRK3 and RK4, and three ARKIMEX schemes, ARKIMEX2C, ARKIMEX3 and ARKIMEX4 (four-stage, fourth-order). The methods converge at their theoretical convergence rates. Figure 2(b) shows the error in mass conservation for the various methods and time-step sizes. Mass is conserved to round-off error for all the methods considered.

5 Conclusions

A high-order accurate finite-difference method for the simulation of atmospheric flows is proposed in this paper. The algorithm uses the CRWENO scheme for spatial discretization and the ARKIMEX schemes for time integration. The high spectral resolution of the CRWENO scheme allows the accurate modeling of all relevant length scales, while maintaining nonoscillatory behavior across regions of strong gradients. The ARKIMEX methods split the governing equations into its stiff and non-stiff components and integrates them with implicit and explicit multi-stage Runge-Kutta schemes respectively. Thus, the time step size is not restricted by the acoustic waves. The algorithm is applied to a benchmark atmospheric flow problem and solutions show excellent agreement with existing results in the literature. The split implicit-explicit time-integrators show optimal convergence when coupled with the nonlinear finite-difference scheme and do not violate mass conservation.

Acknowledgements This material is based upon work supported by the U.S. Department of Energy, Office of Science, Advanced Scientific Computing Research, under contract DE-AC02-06CH11357.

References

1. Ahmad, N., Lindeman, J.: Euler solutions using flux-based wave decomposition. International Journal for Numerical Methods in Fluids **54**(1), 47–72 (2007). DOI 10.1002/fld.1392
2. Ascher, U.M., Ruuth, S.J., Spiteri, R.J.: Implicit-explicit Runge-Kutta methods for time-dependent partial differential equations. Applied Numerical Mathematics **25**(2-3), 151–167 (1997). DOI 10.1016/S0168-9274(97)00056-1
3. Balay, S., Brown, J., Buschelman, K., Eijkhout, V., Gropp, W.D., Kaushik, D., Knepley, M.G., McInnes, L.C., Smith, B.F., Zhang, H.: PETSc Users Manual. Tech. Rep. ANL-95/11 - Revision 3.4, Argonne National Laboratory (2013)
4. Balay, S., Brown, J., Buschelman, K., Gropp, W.D., Kaushik, D., Knepley, M.G., McInnes, L.C., Smith, B.F., Zhang, H.: PETSc Web page (2013). http://www.mcs.anl.gov/petsc
5. Ghosh, D., Baeder, J.D.: Compact reconstruction schemes with weighted ENO limiting for hyperbolic conservation laws. SIAM Journal on Scientific Computing **34**(3), A1678–A1706 (2012). DOI 10.1137/110857659
6. Ghosh, D., Baeder, J.D.: Weighted non-linear compact schemes for the direct numerical simulation of compressible, turbulent flows. Journal of Scientific Computing **61**(1), 61–89 (2014). DOI 10.1007/s10915-014-9818-0
7. Ghosh, D., Constantinescu, E.M., Brown, J.: Efficient implementation of nonlinear compact schemes on massively parallel platforms. Submitted
8. Ghosh, D., Medida, S., Baeder, J.D.: Application of compact-reconstruction weighted essentially nonoscillatory schemes to compressible aerodynamic flows. AIAA Journal **52**(9), 1858–1870 (2014). DOI 10.2514/1.J052654
9. Giraldo, F., Kelly, J., Constantinescu, E.: Implicit-explicit formulations of a three-dimensional nonhydrostatic unified model of the atmosphere (NUMA). SIAM Journal on Scientific Computing **35**(5) (2013). DOI 10.1137/120876034
10. Giraldo, F., Restelli, M., Lauter, M.: Semi-implicit formulations of the Navier-Stokes equations: Application to nonhydrostatic atmospheric modeling. SIAM Journal on Scientific Computing **32**(6), 3394–3425 (2010). DOI 10.1137/090775889
11. Jiang, G.S., Shu, C.W.: Efficient implementation of weighted ENO schemes. Journal of Computational Physics **126**(1), 202–228 (1996). DOI http://dx.doi.org/10.1006/jcph.1996.0130
12. Kennedy, C.A., Carpenter, M.H.: Additive Runge-Kutta schemes for convection-diffusion-reaction equations. Applied Numerical Mathematics **44**(1-2), 139–181 (2003). DOI 10.1016/S0168-9274(02)00138-1
13. Klemp, J.B., Skamarock, W.C., Dudhia, J.: Conservative split-explicit time integration methods for the compressible nonhydrostatic equations. Monthly Weather Review **135**, 28972913 (2007). DOI 10.1175/MWR3440.1
14. Lee, C., Seo, Y.: A new compact spectral scheme for turbulence simulations. Journal of Computational Physics **183**(2), 438–469 (2002). DOI http://dx.doi.org/10.1006/jcph.2002.7201
15. Lele, S.K.: Compact finite difference schemes with spectral-like resolution. Journal of Computational Physics **103**(1), 16–42 (1992). DOI http://dx.doi.org/10.1016/0021-9991(92)90324-R
16. LeVeque, R.J.: Finite Volume Methods for Hyperbolic Problems. Cambridge Texts in Applied Mathematics. Cambridge University Press (2002)
17. Liu, X.D., Osher, S., Chan, T.: Weighted essentially non-oscillatory schemes. Journal of Computational Physics **115**(1), 200–212 (1994). DOI http://dx.doi.org/10.1006/jcph.1994.1187
18. Nagarajan, S., Lele, S.K., Ferziger, J.H.: A robust high-order compact method for large eddy simulation. Journal of Computational Physics **191**(2), 392–419 (2003). DOI http://dx.doi.org/10.1016/S0021-9991(03)00322-X
19. Pareschi, L., Russo, G.: Implicit-explicit Runge-Kutta schemes and applications to hyperbolic systems with relaxation. Journal of Scientific Computing **25**(1-2), 129–155 (2005). DOI 10.1007/BF02728986